Quantum phase transition and interference trapping of populations in a coupled-resonator waveguide

Lei Qiao,[1] Ya-Ju Song,[1] and Chang-Pu Sun[1,2,*]
[1]*Graduate School of Chinese Academy of Engineering Physics, Beijing 100084, China*
[2]*Beijing Computational Science Research Center, Beijing 100193, China*

(Received 21 February 2019; published 15 July 2019)

We study the energy structure and dynamics of a V-type three-level emitter embedded in a one-dimensional waveguide with model dispersion. Due to the presence of two different couplings between the upper levels and the waveguide modes, we find that the bound states in this system are quite different from the case of a two-level emitter. The energy structure is dependent on the relative position of the emitter's transition frequencies from the band with finite width. We obtain the phase diagrams through numerical analysis. The dynamics of spontaneous emission of the system is calculated exactly in the general case by means of the Green's function approach. The emitted photon is characterized by two components: a localized part and a traveling part, and the average frequency of the traveling part is different from that for resonant scattering. Through the quantum interference between the emitter's two transitions, it is found that the total excitation number of the localized photon and emitter can be greatly enhanced in some case in the spontaneous-emission process.

DOI: 10.1103/PhysRevA.100.013825

I. INTRODUCTION

Motivated by the experimental progress in quantum communication, quantum computation, and quantum information processes, much attention has been paid to the study of light-matter interaction in waveguiding structures in recent years [1–8]. These waveguiding structures can be realized in many different ways, such as the surface plasmons confined on a conducting nanowire coupled to a single two-level emitter [9], a one-dimensional superconducting transmission line coupled to a single artificial atom [10], or a photonic nanowire with an embedded quantum dot [11]. For that the coupled-resonator waveguide (CRW) with good scalability and integrability has become available recently [12–16], light-matter interaction in one-dimensional CRWs with different local coupled quantum systems has extensively been studied, and many different quantum devices have been proposed theoretically based on the rich physics in these systems, such as the controllable quantum switches [2,17–20], single-photon routers [21,22], photon memory device [23], and controllable frequency converters [24].

For the CRW locally coupled by a two-level system (TLS) which is known as one of the general Fano-Anderson models, it has been demonstrated that there are two bound states localized near around the TLS, whose energies lie outside the finite band of bath modes [25,26]. As the coupling strength between TLS and waveguide mode increases, these bound states' energies get away from the band. Due to the presence of atom-photon bound states, the excitation of TLS cannot be transformed entirely into the field and thus exhibits a fractional decay [27]. Some aspects of such bound states have been discussed in the photon scattering problems [28–31]. In the study of spontaneous emission, it was found that the population in the excited state of TLS experiences from exponential decay to Rabi oscillations when the coupling strength becomes from weak to strong due to the existence of these bound states [32] and there is an energy shift of the emitted photon with respect to the energy required to excite the TLS [33].

In this paper, we focus on the CRW which is locally coupled by a three-level atom (TLA). The two upper levels of the atom are coupled by the same waveguide mode to the lower level. Different from the case of TLS that there are always two bound states no matter whether the coupling strength is weak or strong, we find that there is a transition of the number of bound states when the two coupling strengths between the TLA and the waveguide mode vary. The change of the energy level structure reveals that there is a quantum phase transition in this process. Because of the presence of these bound states, the populations in the upper levels will not totally decay to zero in the spontaneous emission process [27]. Such population trapping exists in the form of a residual oscillatory behavior of each excitation at long enough time when at least two bound states go into effect and in the form of an approximate constant without oscillation when only one bound state plays the main role. We investigate how the quantum interference between the two transitions of three-level atom affects the time evolution of the populations. It is found that the population trapping can be greatly enhanced in four cases by controlling the initial state: (i) the energy band is narrow; (ii) the two transition frequencies of atom are much greater than scattering energy; (iii) the two transition frequencies are equal to each other; (iv) the scattering energy is much greater than the two transition frequencies.

The paper is organized as follows. In Sec. II, we introduce the model of coupled-resonator waveguide coupled by a

*cpsun@csrc.ac.cn

three-level atom. In Sec. III, we calculate the system's stationary states, both the bound ones and the scattering ones, through the method of the Green's function. In Sec. IV, we study the poles of the Green's function and investigate the system's eigenvalues. In Sec. V, we use the bound and the scattering states to study the atom's spontaneous emission by focusing on the time evolution of the population in the upper levels. In Sec. VI, we use the bound and the scattering states to study the atom's spontaneous emission by focusing on the time evolution of photon probability distribution and analyze the localized radiation field. Finally, we summarize the results and give the conclusions in Sec. IV.

II. MODEL

As shown in Fig. 1, the system we consider consists of a coupled-resonator waveguide with a three-level atom coupled at site $x = x_0$. The atom is characterized by a ground state $|g\rangle$ and two excited states $|e_1\rangle$, $|e_2\rangle$. Denote $a_x^\dagger$ (a_x) as the creation (annihilation) operator of the waveguide mode at position x; then the Hamiltonian of the system can be written as (with $\hbar = 1$)

$$H = \sum_{x=1}^{N} \omega a_x^\dagger a_x - J \sum_{x=1}^{N-1} (a_{x+1}^\dagger a_x + a_x^\dagger a_{x+1}) + \sum_{i=1,2} \left[\Omega_i |e_i\rangle\langle e_i| + V_i\left(\sigma_i^+ a_{x_0} + \sigma_i^- a_{x_0}^\dagger\right)\right], \quad (1)$$

where ω is the on-site energy of each resonator. J represents the hopping energy of the photon between two neighbor sites. Here, we set the ground energy of the atom to be zero as reference and the resonant transition frequencies of two excited states are represented by Ω_1 and Ω_2. $\sigma_i^+ = |e_i\rangle\langle g|$ ($\sigma_i^- = |g\rangle\langle e_i|$) is the raising (lowering) operator acting onto the atom. V_1 and V_2 are the coupling strength between waveguide mode and each excited state. Here, l is the lattice constant so that the system's total length is $L = Nl$. For simplicity, we assume l to be unity in the following. When one of the atom's transition frequencies and its corresponding coupling strength are taken to be the limit $\Omega_i/J, V_i/J \to 0$ ($i = 1$ or 2), the Hamiltonian will reduce to the case of a two-level atom [2].

By introducing the momentum representation of the annihilation operator

$$a_k = \frac{1}{\sqrt{N}} \sum_x e^{ikx} a_x, \quad (2)$$

where $k \in [-\pi, \pi]$ is the wave number within the first Brillouin zone, the free-photon Hamiltonian is written as $\sum_k \omega_k a_k^\dagger a_k$ with the dispersion relation

$$\omega_k = \omega - 2J\cos(k). \quad (3)$$

This mode frequency is inside a scattering energy band with width $4J$, which is centered around the on-site energy ω. Thus, in the momentum space, the Hamiltonian in Eq. (1) can be written as

$$H = H_0 + V, \quad (4)$$

with

$$H_0 = \sum_k \omega_k a_k^\dagger a_k + \sum_i \Omega_i |e_i\rangle\langle e_i| \quad (5)$$

and

$$V = \sum_i \frac{V_i}{\sqrt{N}} \sum_k (\sigma_i^+ a_k + \sigma_i^- a_k^\dagger), \quad (6)$$

which shows that the three-level atom is coupled to a finite energy band of waveguide modes. Here, for simplicity, we take the site x_0 as zero point.

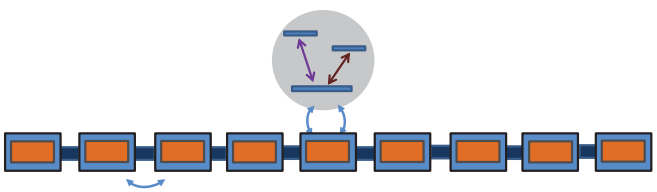

FIG. 1. Scheme of the system. A one-dimensional coupled-resonator waveguide is coupled by a three-level atom.

III. BOUND STATES AND SCATTERING STATES

The spectrum of the system contains a continuum of scattering states whose energies lie inside a finite band and discrete levels of bound states. The case of scattering states has been studied in the literature [21,24]. In this section, we show how to derive the bound states and scattering states of the system with the Green's function approach [34,35]. It is worth noting that the result of CRW coupled by a two-level atom has been presented in the paper [32], which only considers the case that a two-level atom is on resonance with the zeroth cavity, i.e., the transition frequency of the two-level atom coincides with on-site energy ω. Here, we consider the general situation with a three-level atom.

The Green's function is defined in terms of Hamiltonian H as [35]

$$\hat{G}(z) = \frac{1}{z - H}, \quad (7)$$

where z is a complex energy variable. $\hat{G}(z)$ is an analytic function in the complex z plane except at those points or portions of the real z axis that correspond to the eigenvalues of H. Besides, $\hat{G}(z)$ satisfies the resolvent equation [36]

$$\hat{G}(z) = \hat{G}_0(z) + \hat{G}_0(z) V \hat{G}(z) = \hat{G}_0(z) + \hat{G}(z) V \hat{G}_0(z). \quad (8)$$

Here, $\hat{G}_0(z)$ is the free Green's function and is defined as

$$\hat{G}_0(z) = \frac{1}{z - H_0}. \quad (9)$$

The pole of $\hat{G}_0(z)$ gives the eigenvalues of free Hamiltonian H_0.

A. Bound states

We will first calculate the matrix elements of $\hat{G}(z)$: $\langle 0, e_i|\hat{G}(z)|0, e_j\rangle$, $\langle 0, e_i|\hat{G}|k, g\rangle$, and $\langle p, g|\hat{G}|k, g\rangle$ ($i, j = 1, 2$), where $|0, e_j\rangle$ represents that there is zero photon in the

waveguide and the atom is in the excited state $|e_j\rangle$, while $|k, g\rangle$ indicates that the atom is in its ground state and one photon with momentum k exists. Note that both $|0, e_j\rangle$ and $|k, g\rangle$ are the eigenvalues of H_0. Since $G_0(z)$ is associated with Hamiltonian H_0, the matrix elements can be easily calculated as

$$\langle 0, e_i|\hat{G}_0(z)|0, e_j\rangle = \frac{\delta_{i,j}}{z-\Omega_j}, \tag{10}$$

$$\langle 0, e_i|\hat{G}_0(z)|k, g\rangle = 0, \tag{11}$$

$$\langle p, g|\hat{G}_0(z)|k, g\rangle = \frac{\delta_{p,k}}{z-\omega_k}. \tag{12}$$

Here, $\langle p, g|\hat{G}_0(z)|k, g\rangle$ has a pole inside the band of the eigenvalues of H_0. Additionally, the identity operator in a single excited sector is given by

$$\mathbf{I}_1 = \sum_k |k, g\rangle\langle k, g| + |0, e_1\rangle\langle 0, e_1| + |0, e_2\rangle\langle 0, e_2|. \tag{13}$$

By sandwiching the right side of Eqs. (8) with the identity operator $\mathbf{I}_1$ and inserting the identity operator between V and $\hat{G}$, also using Eqs. (10), (11), and (12), one can obtain the self-consistent equations

$$\langle 0, e_i|\hat{G}|k, g\rangle = \sum_j \frac{V_j\langle 0, e_i|\hat{G}|0, e_j\rangle}{\sqrt{N}(z-\omega_k)}, \tag{14}$$

$$\langle 0, e_i|\hat{G}|0, e_j\rangle = \sum_k \frac{V_j\langle 0, e_i|\hat{G}|k, g\rangle}{\sqrt{N}(z-\Omega_j)} \quad (i \neq j), \tag{15}$$

$$\langle 0, e_i|\hat{G}|0, e_i\rangle = \langle 0, e_i|\hat{G}_0|0, e_i\rangle + \sum_k \frac{V_i\langle 0, e_i|\hat{G}|k, g\rangle}{\sqrt{N}(z-\Omega_i)}, \tag{16}$$

$$\langle p, g|\hat{G}|k, g\rangle = \frac{\delta_{p,k}}{z-\omega_k} + \sum_i \frac{V_i\langle p, g|\hat{G}|0, e_i\rangle}{\sqrt{N}(z-\omega_k)}. \tag{17}$$

Taking Eqs. (15) and (16) into the expression of $\langle 0, e_i|\hat{G}|k, g\rangle$ and after some calculation, $\langle 0, e_i|\hat{G}|k, g\rangle$ can be exactly solved as

$$\langle 0, e_i|\hat{G}|k, g\rangle = \frac{V_i(z-\Omega_1)(z-\Omega_2)}{\sqrt{N}(z-\omega_k)(z-\Omega_i)K(z)}, \tag{18}$$

where $K(z) = (z-\Omega_1)(z-\Omega_2) - (z-\Omega_1)V_2^2 I(z) - (z-\Omega_2)V_1^2 I(z)$ and $I(z) = \sum_k 1/[N(z-\omega_k)]$. The function $I(z)$ is analytic in the whole complex plane except a branch cut on the real axis from $\omega - 2J$ to $\omega + 2J$. In this branch cut region $I(z)$ is divergent and not well defined. With this result of $\langle 0, e_i|\hat{G}|k, g\rangle$, the solutions to other matrix elements can be derived

$$\langle 0, e_1|\hat{G}|0, e_1\rangle = \frac{z-\Omega_2-V_2^2 I(z)}{K(z)}, \tag{19}$$

$$\langle 0, e_1|\hat{G}|0, e_2\rangle = \frac{V_1 V_2 I(z)}{K(z)}, \tag{20}$$

$$\langle 0, e_2|\hat{G}|0, e_2\rangle = \frac{z-\Omega_1-V_1^2 I(z)}{K(z)}, \tag{21}$$

$$\langle p, g|\hat{G}|k, g\rangle = \frac{\delta_{p,k}}{z-\omega_k} + \frac{U(z)(z-\Omega_1)(z-\Omega_2)}{N(z-\omega_p)(z-\omega_k)K(z)}, \tag{22}$$

where $U(z) = \sum_i V_i^2/(z-\Omega_i)$. Note that $|0, e_j\rangle$ and $|k, g\rangle$ are the eigenvalues of H_0 but not that of H. So the system's bound-state energy can be given out by the common poles of these matrix elements of $\hat{G}$ [35]:

$$(E-\Omega_1)(E-\Omega_2) = \left[(E-\Omega_1)V_2^2 + (E-\Omega_2)V_1^2\right]I(E). \tag{23}$$

The stationary states $|\Psi_n\rangle$ associated with the discrete eigenvalues E_n of H obey the Schrödinger equation $H|\Psi_n\rangle = E_n|\Psi_n\rangle$. These eigenvalues are given by Eq. (23). According to the properties of the Green's function, the residue of matrix elements $\langle\_|\hat{G}(z)|\_\rangle$ with $z = E_n$ corresponds to the matrix elements $\langle\_|\Psi_n\rangle\langle\Psi_n|\_\rangle$. Here, $|\_\rangle$ can be chosen as $|0, e_j\rangle$ or $|k, g\rangle$ because these elements of $\hat{G}$ have been solved above. By this relation, one can obtain the states $|\Psi_n\rangle$

$$|\Psi_n\rangle = \left\{\sum_k \frac{\sqrt{(z-\Omega_1)(z-\Omega_2)}}{\sqrt{N}(z-\omega_k)\sqrt{I(z)[K(z)]'}}|k, g\rangle + \frac{\sqrt{(z-\Omega_2)-V_2^2 I(z)}}{\sqrt{[K(z)]'}}|0, e_1\rangle + \frac{\sqrt{(z-\Omega_1)-V_1^2 I(z)}}{\sqrt{[K(z)]'}}|0, e_2\rangle\right\}|_{z=E_n}, \tag{24}$$

where $[K(z)]'$ means the derivative of $K(z)$ with respect to z.

B. Scattering states

Now, we consider the photon scattering in the waveguide system. As mentioned above, the scattering-state eigenvalue, which is continuous spectrum, corresponds to a branch cut of $\langle p, g|\hat{G}|k, g\rangle$ and is inside the band $(\omega - 2J, \omega + 2J)$. The scattering state $|\Psi_k\rangle$ is related to the input state $|k, g\rangle$ via the Lippmann Schwinger equation

$$|\Psi_k\rangle = |k, g\rangle + G^+(\omega_k)\hat{V}|k, g\rangle, \tag{25}$$

where $G^+(\omega_k) = \lim_{\delta\to 0^+} G(\omega_k + i\delta)$. With the solved matrix elements of $\hat{G}$ in Eqs. (18)–(22), $|\Psi_k\rangle$ can be calculated as

$$|\Psi_k\rangle = |k, g\rangle + \sum_{k'} \frac{u_{kk'}}{F_k}|k', g\rangle + \frac{u_{ke_1}}{\sqrt{N}F_k}|0, e_1\rangle + \frac{u_{ke_2}}{\sqrt{N}F_k}|0, e_2\rangle, \tag{26}$$

where $u_{kk'} = \{V_1^2(\omega_k - \Omega_2) + V_2^2(\omega_k - \Omega_1)\}/\{N(\omega_k + i\delta - \omega_{k'})\}$, $u_{ke_1} = V_1(\omega_k - \Omega_2)$, $u_{ke_2} = V_2(\omega_k - \Omega_1)$, and

$$F_k = (\omega_k - \Omega_1)(\omega_k - \Omega_2) + i\frac{u_{ke_1}V_1 + u_{ke_2}V_2}{2J|\sin(k)|}. \tag{27}$$

Inserting the identity operator $\mathbf{I}_2 = \sum_x |x, g\rangle\langle x, g| + |0, e_1\rangle\langle 0, e_1| + |0, e_2\rangle\langle 0, e_2|$ into the right side of Eq. (26), the scattering state $|\Psi_k\rangle$ can be rewritten as

$$|\Psi_k\rangle = \sum_x u_{kx}|x, g\rangle + \frac{u_{ke_1}}{\sqrt{N}F_k}|0, e_1\rangle + \frac{u_{ke_2}}{\sqrt{N}F_k}|0, e_2\rangle, \tag{28}$$

where $u_{kx} = \frac{1}{\sqrt{N}}\{e^{ikx} + r_k e^{i|kx|}\}$ is the probability amplitude in position space and

$$r_k = -i\frac{V_1^2(\omega_k - \Omega_2) + V_2^2(\omega_k - \Omega_1)}{|2J\ \sin(k)|F_k} \tag{29}$$

is the photon reflection amplitude, while $t_k = 1 + r_k$ represents the transmission amplitude. r_k and t_k satisfy the relation $|r_k|^2 + |t_k|^2 = 1$.

IV. QUANTUM PHASE TRANSITION

For the case of the waveguide system with a two-level atom, there are always two discrete poles in the Green's function which correspond to two bound states [25]. One is above the top of the scattering energy band, while the other is below the bottom of the band. However, the case for a three-level atom is different. In this section, we will show that how the quantum phase transition happens when the values of coupling strength V_1, V_2 changes with different transition frequencies Ω_1, Ω_2.

Now we investigate the poles of the Green's function as presented in Eq. (23). As mentioned above, the function $I(z)$ is not well defined when z is inside the scattering band. However, when z is infinitely close to the range $[\omega - 2J, \omega + 2J]$ from the whole complex plane, $I(z)$ can be calculated as $I(z) = -2\pi i/\sqrt{4J^2 - z^2}$ if $\lim_{\delta\to 0^+}(z - i\delta) \in [\omega - 2J, \omega + 2J]$, while $I(z) = 2\pi i/\sqrt{4J^2 - z^2}$ if $\lim_{\delta\to 0^+}(z + i\delta) \in [\omega - 2J, \omega + 2J]$. With this limit equation, no solutions are found in Eq. (23) except a special situation that the values of Ω_1, Ω_2 are equal, i.e., $\Omega_1 = \Omega_2 = \Omega$. In this case, we found $E = \Omega$ is the solution to Eq. (23). Now we focus on the region outside the band. In this case, Eq. (23) is calculated as

$$(E - \Omega_1)(E - \Omega_2) = \frac{(E - \Omega_1)V_2^2 + (E - \Omega_2)V_1^2}{(E - \omega)\sqrt{1 - \frac{4J^2}{(E-\omega)^2}}}. \tag{30}$$

The number of eigenvalues depends on the relative positions between Ω_1, Ω_2 and the scattering band. Without loss of generality, we assume $\Omega_1 > \Omega_2$ in the paper. If the two transition frequencies Ω_1, Ω_2 are outside the band and are in the same side, i.e., $\Omega_1, \Omega_2 > \omega + 2J$ or $\Omega_1, \Omega_2 < \omega - 2J$, the equation always has three eigenvalues which correspond to three bound states. However, if Ω_1, Ω_2 are outside the band and are in the different side, i.e., $\Omega_1 > \omega + 2J$ and $\Omega_2 < \omega - 2J$, there will be two or three solutions to the equation. It depends on the value of $h(V_1, V_2) \equiv (\Omega_1 V_2^2 + \Omega_2 V_1^2)/(V_1^2 + V_2^2)$. When $|h(V_1, V_2) - \omega| < 2J$, two roots exist in Eq. (30); otherwise, there will be three roots. On another hand, if one of the frequencies is inside the band and the other is outside, for example, $\Omega_2 \in [\omega - 2J, \omega + 2J]$ and $\Omega_1 > \omega + 2J$, there are also two different cases. When $h(V_1, V_2) < \omega + 2J$, two roots exist; otherwise, the equation has three roots. At last, we discuss that both Ω_1 and Ω_2 are inside the band. In this situation, due to the value of $h(V_1, V_2)$ always being in the region of the scattering band, only two roots exist in the equation.

In Fig. 2(a), we plot the bound-state energies as a function of the coupling strength V_1 in the case that Ω_2 is inside the region $[\omega - 2J, \omega + 2J]$ and Ω_1 is outside. One can see that the energies of bound states lie on both sides of the band. As

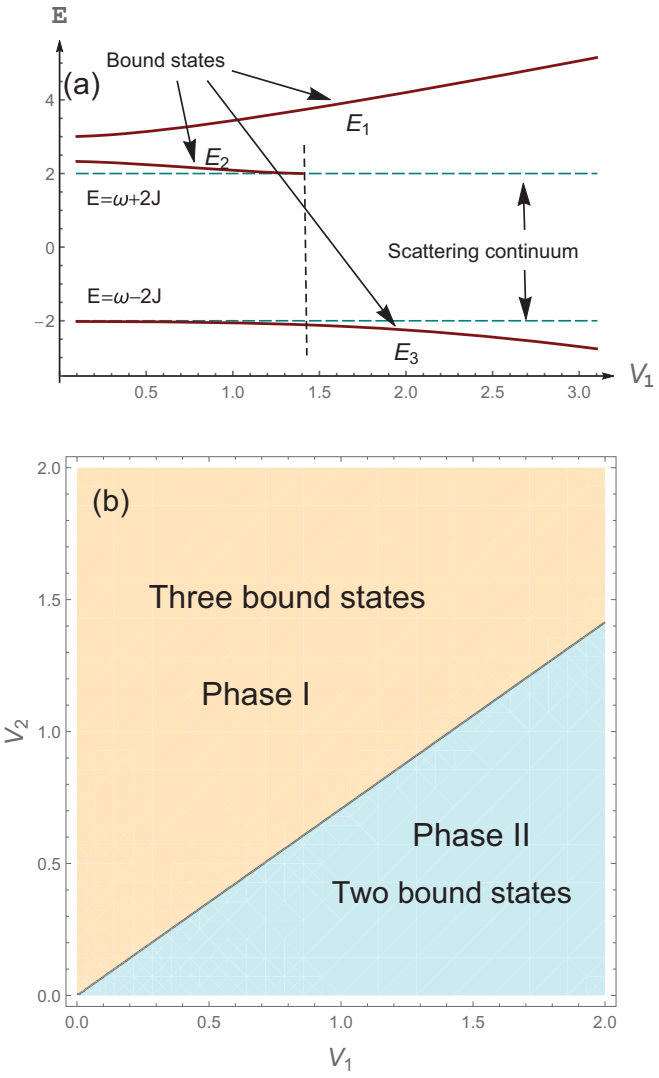

FIG. 2. (a) Energy spectrum as a function of the atom-photon coupling strength V_1. Another coupling strength $V_2 = 1$. (b) Phase diagram of the system in the V_1-V_2 plane. The transition frequencies $\Omega_1 = 3$, $\Omega_2 = 1.5$ and the center energy of scattering band $\omega = 0$. All of the energies are in units of J.

the coupling strength V_1 increases, E_1 (E_3) comes away from the top (bottom) of the band. But E_2 gets closer to the band top. At about $V_1 = 1.42J$, E_2 disappears and the number of bound states of the system becomes from three to two. Further research shows that if the value of V_1 is fixed, for example, $V_1 = J$, and the coupling strength V_2 varies, other parameters are the same as that in Fig. 2(a); we found that there are two bound states when V_2 is small ($V_2 < 0.89J$). When V_2 increases and is greater than $0.89J$, the middle bound state E_2 appears and gets away from the top of the band. In Fig. 2(b), we show the phase diagram of the system in the V_1-V_2 plane. One can clearly see the different phase when V_1, V_2 change.

V. POPULATIONS IN THE TWO UPPER LEVELS

We now study the dynamics of the coupled-resonator waveguide coupled by a three-level atom. To study the time

evolution of the system's wave function, we express the wave function expanded by all the bound states and the scattering states, which construct a set of complete basis

$$|\Psi(t)\rangle = \sum_k B_k e^{-i\omega_k t}|\Psi_k\rangle + \sum_n B_n e^{-iE_n t}|\Psi_n\rangle. \tag{31}$$

From the initial state $|\Psi(0)\rangle = A_1(0)|0, e_1\rangle + A_2(0)|0, e_2\rangle + \sum_k C_k(0)|k, g\rangle$ with $|A_1(0)|^2 + |A_2(0)|^2 = 1$ and $C_k(0) = 0$, we obtain

$$B_k = \frac{u_{ke_1}A_1(0) + u_{ke_2}A_2(0)}{\sqrt{N}F_k^*} \tag{32}$$

and

$$B_n = \frac{\sqrt{(z-\Omega_2) - V_2^2 I(z)}A_1(0)}{\sqrt{[K(z)]'}}\bigg|_{z=E_n} + \frac{\sqrt{(z-\Omega_1) - V_1^2 I(z)}A_2(0)}{\sqrt{[K(z)]'}}\bigg|_{z=E_n}. \tag{33}$$

With the expression of $|\Psi(t)\rangle$, the system's average energy can be obtained as $\langle H\rangle = \sum_k |B_k|^2\omega_k + \sum_n |B_n|^2 E_n$. According to the energy conservation, $\langle H\rangle$ is always equal to the initial total energy $E_{tot} = |A_1(0)|^2\Omega_1 + |A_2(0)|^2\Omega_2$. It can be seen that due to the presence of bound states, the energy of the emitted field is different from the total energy E_{tot}. When the initial amplitude $A_2(0)$ is taken to be zero, i.e., $E_{tot} = \Omega_1$, the amount of energy that transfers to the emitted field will produce a shift from Ω_1.

The population in the upper level $|0, e_1\rangle$ is derived as

$$A_1(t) = \langle 0, e_1|\Psi(t)\rangle = \sum_n \frac{(z-\Omega_2)A_1(0) + I(z)U_1(0)}{[K(z)]'}e^{-izt}\bigg|_{z=E_n} + \int_{-\pi}^{\pi} \frac{\left[u_{ke_1}A_1(0) + u_{ke_2}A_2(0)\right]u_{ke_1}e^{-i\omega_k t}}{2\pi|F_k|^2}dk, \tag{34}$$

where $U_1(0) = V_1V_2A_2(0) - V_2^2A_1(0)$. The first term comes from the bound states while the second term, which represents the nonlocalized photon, comes from the scattering states. Similarly, the population in the upper level $|0, e_2\rangle$ is obtained as

$$A_2(t) = \langle 0, e_2|\Psi(t)\rangle = \sum_n \frac{(z-\Omega_1)A_2(0) + I(z)U_2(0)}{[K(z)]'}e^{-izt}\bigg|_{z=E_n} + \int_{-\pi}^{\pi} \frac{\left[u_{ke_1}A_1(0) + u_{ke_2}A_2(0)\right]u_{ke_2}e^{-i\omega_k t}}{2\pi|F_k|^2}dk, \tag{35}$$

where $U_2(0) = V_1V_2A_1(0) - V_1^2A_2(0)$. From the expression of $A_1(t)$ and $A_2(t)$, one can see that the number and characteristics of these eigenvalues E_n play important roles in the dynamics of spontaneous emission. Also, it can be seen that both $A_1(t)$ and $A_2(t)$ are associated with $A_1(0)$ and $A_2(0)$. This relation reveals the quantum interference between the two transitions of a three-level atom. Besides this type of interference, there is another quantum interference that is between different bound (scattering) states and also between different bound and scattering states. These two types of interference could lead to some new phenomena in the spontaneous emission process.

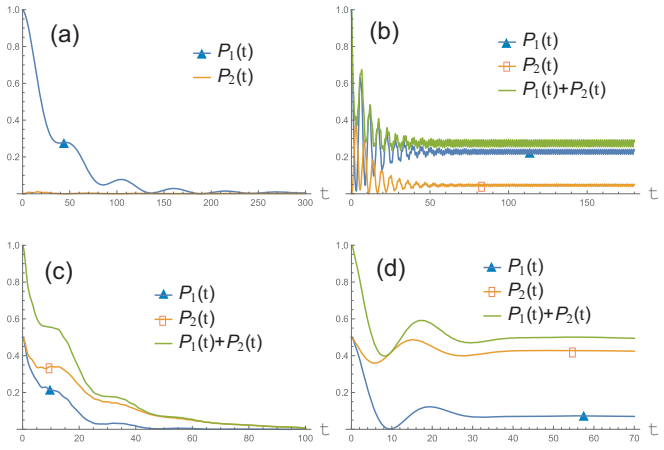

FIG. 3. Time evolution of the atom's upper-level population $P_1(t)$ and $P_2(t)$. The time is in units of $1/J$. (a) $\Omega_1 = 1.9J$, $\Omega_2 = 1.3J$, $V_1 = 0.1J$, $V_2 = 0.3J$. (b) $\Omega_1 = 1.9J$, $\Omega_2 = 1.3J$, $V_1 = 1.0J$, $V_2 = 0.8J$. (c) $\Omega_1 = 0.4J$, $\Omega_2 = 0.1J$, $V_1 = 0.3J$, $V_2 = 0.2J$. (d) $\Omega_1 = 1.9J$, $\Omega_2 = 2.1J$, $V_1 = 0.3J$, $V_2 = 0.2J$. The center energy of scattering band $\omega = 0$.

A. From complete decay to finite trapping

The time evolution of the populations in the two excited states of the atom is determined by

$$P_1(t) = |A_1(t)|^2, \quad P_2(t) = |A_2(t)|^2. \tag{36}$$

Because $A_1(t)$ and $A_2(t)$ are associated with $A_1(0)$ and $A_2(0)$, the population in one upper level can decay to the atom's ground state, and then jump to the other upper level by absorbing the photon emitted in the previous decay process. From Eqs. (34) and (35), we know that the amplitudes $A_1(t)$ and $A_2(t)$ are composed of two terms. The first term, which is formed by localized bound states, presents no decay behavior as time goes on, while the second term, which leads to the formation of an unlocalized propagating field, vanishes as time goes infinite. These two terms result that the spontaneous emission is quite distinct from that in vacuum which is exponential decay. Furthermore, it can be seen that if the two initial amplitudes $A_1(0)$ and $A_2(0)$ are equal, for example, $A_1(0) = A_2(0) = 1/\sqrt{2}$, the ratio of the amplitudes $P_1(t)/P_2(t)$ will be independent of the initial state.

In Figs. 3(a) and 3(b), we study the time evolution of the two upper-level populations with different coupling strengths. The initial amplitudes are assumed as $A_1(0) = 1$, $A_2(0) = 0$. One sees that when the coupling strengths V_1, V_2 are weak, $P_1(t)$ gradually decays to zero as time goes on and $P_2(t)$ increases first, then also finally decays to zero as shown in Fig. 3(a). In this situation, the role of bound states is not important. However, as the coupling strengths V_1, V_2 increase, the bound states could become important. In Fig. 3(b), it is shown that $P_1(t)$ decays fast at first, then increases and

redecays, while $P_2(t)$ increases first, then decays and reincreases. Finally, $P_1(t)$ and $P_2(t)$ tends to stable oscillation with a nonzero value. The sum of $P_1(t)$ and $P_2(t)$ also tends to stable oscillation as time goes infinite. This oscillation reveals that a photon, which is localized near the atom, is cyclically emitted and absorbed by the atom. It can be seen that due to the existence of localized bound states, a fractional population is trapped in the two upper levels.

Besides increasing the coupling strength, we find that the difference between transition frequency Ω_i (i, $j = 1, 2$) and on-site energy ω also affects the trapping of population. In Figs. 3(c) and 3(d), the time evolution of the two upper-level populations is plotted with different transition frequencies. Like that in Fig. 3(a), the two populations in Fig. 3(c) decay to zero when Ω_i is not far from the center energy ω. As the value of $|\Omega_i - \omega|$ becomes large as shown in Fig. 3(d), fractional populations are trapped in the excited states even when the coupling strengths V_1, V_2 are weak. Further research shows that the trapping can be obviously enhanced when the transition frequency Ω_i increased to outside the scattering energy band.

Finally, we analyze the result when the time goes long enough. In this case, the populations $P_1(t)$ and $P_2(t)$ tend to

$$P_1(t) = \sum_n |\alpha_n|^2 + \sum_{n\neq m} \alpha_n^* \alpha_m e^{-i(E_m - E_n)t}, \tag{37}$$

$$P_2(t) = \sum_n |\beta_n|^2 + \sum_{n\neq m} \beta_n^* \beta_m e^{-i(E_m - E_n)t}, \tag{38}$$

where $\alpha_n = (z - \Omega_2)A_1(0) + I(z)U_1(0)/[K(z)]'|_{z=E_n}$ and $\beta_n = (z - \Omega_1)A_2(0) + I(z)U_2(0)/[K(z)]'|_{z=E_n}$. The second term in $P_1(t)$ and $P_2(t)$ represents the interferences between different bound states. Usually, these interferences lead to the oscillatory behavior of $P_1(t)$ and $P_2(t)$ when time is enough long. This is why $P_1(t)$ and $P_2(t)$ in Fig. 3(b) present periodic oscillation at last. However, we find that in some situations, for example, the situation given by Fig. 3(d), only one bound state plays the main role in the spontaneous emission process and the other bound states could be approximately neglected. In these situations, $P_1(t)$ and $P_2(t)$ will decay to a finite constant without oscillation when time goes infinite. Specifically, for example, with the given parameters in Fig. 3(d), the coefficient B_n in Eq. (31) is obtained as $|B_1|^2 = 0.650150$, which is much greater than $|B_2|^2 = 0.000195$ and $|B_3|^2 = 0.000130$ (B_1, B_2, B_3 correspond to the eigenvalues E_1, E_2, E_3, respectively, and $E_1 > E_2 > E_3$). So only the bound state with energy being E_1 plays a role and leads to the population trapping at long enough time.

B. Interference trapping

From Fig. 3, we see that the populations in the two upper levels will not decay to zero as time goes to infinity when the coupling strengths are not weak or the frequencies are relatively far from the center energy ω. This trapping effect takes place due to the existence of localized bound states. We call it bound-state trapping here. This type of trapping is also found in the coupled-resonator waveguide with a two-level atom [32] and also in traditional optical lattice system [27].

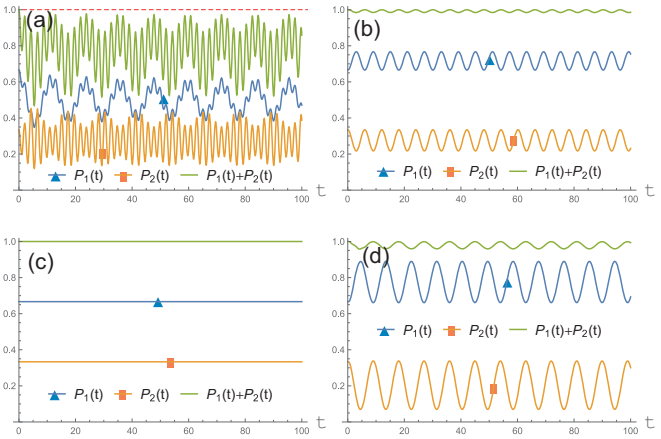

FIG. 4. Time evolution of the atom's upper-level population $P_1(t)$ and $P_2(t)$. (a) $\Omega_1/\omega = 0.2$, $\Omega_2/\omega = 2.6$, $V_1/\omega = 1/(2\sqrt{3})$, $V_2/\omega = \sqrt{2}/\sqrt{3}$, $J/\omega = 0.2$. (b) $\Omega_1/J = 7$, $\Omega_2/J = 8$, $V_1/J = 1/\sqrt{3}$, $V_2/J = \sqrt{2}/\sqrt{3}$, $\omega/J = 0$. (c) $\Omega_1/J = 1$, $\Omega_2/J = 1$, $V_1/J = 1/\sqrt{3}$, $V_2/J = \sqrt{2}/\sqrt{3}$, $\omega/J = 0$. (d) $\Omega_1/J = 1.9$, $\Omega_2/J = 1.3$, $V_1/J = 1/\sqrt{3}$, $V_2/J = \sqrt{2}/\sqrt{3}$, $\omega/J = 6$. For (a), the time is in units of $1/\omega$. For (b)–(d), the time is in units of $1/J$.

In the present system, we found that, by controlling the initial amplitudes of $|0, e_1\rangle$ and $|0, e_2\rangle$, one can trap the determined momentum mode. In the expression of $A_1(t)$ and $A_2(t)$ in Eqs. (34) and (35), both the integrands of scattering items are proportional to $u_{ke_1}A_1(0) + u_{ke_2}A_2(0)$. A complete interference can result in $u_{ke_1}A_1(0) + u_{ke_2}A_2(0) = 0$ as $A_1(0)/A_2(0) = -V_2(\omega_k - \Omega_1)/[V_1(\omega_k - \Omega_2)]$. In this case, the nonlocalized field will not include the momentum with k mode. It can be seen more clearly in the expression of B_k in Eq. (32). The initial amplitudes lead to $B_k = 0$; thus the k-mode photon is not included in the propagation field. In addition, there are four cases in which almost all k-mode photons can be trapped near to the three-level atom: (i) the width of the scattering band is narrow so that ω_k can be considered as $\omega_k \approx \omega$; (ii) the two transition frequencies Ω_1, Ω_2 are much greater than all ω_k; (iii) the two transition frequencies Ω_1, Ω_2 are equal to each other; (iv) all ω_k are much greater than Ω_1 and Ω_2. For case (i), if the initial amplitudes $A_1(0)$ and $A_2(0)$ satisfy $A_1(0)/A_2(0) = -V_2(\omega - \Omega_1)/[V_1(\omega - \Omega_2)]$, the coefficient B_k with different k is approximately equal to zero, so almost no nonlocalized photon is emitted in the spontaneous emission process. For case (ii), if $A_1(0)$, $A_2(0)$ are provided as $A_1(0)/A_2(0) = -V_2\Omega_1/(V_1\Omega_2)$, B_k can also be approximately seen as zero, so nearly no nonlocalized field is emitted. For case (iii), when $A_1(0)/A_2(0) = -V_2/V_1$, the coefficient B_k is exactly zero. In such condition, the amplitudes in the two upper levels will always keep the initial state (see the following). For the last case, no nonlocalized photon is emitted when $A_1(0)$, $A_2(0)$ satisfy the same relation as that in case (iii), i.e., $A_1(0)/A_2(0) = -V_2/V_1$. Because this type of trapping is associated with the interference between two upper levels to the atom's ground state, we call it interference trapping.

In Fig. 4, we investigate the time evolution of the populations of the atom's upper levels for the four interference-trapping cases. Figures 4(a), 4(b), 4(c), and 4(d) correspond to the cases (i), (ii), (iii), and (iv), respectively. In Fig. 4(a),

the initial amplitudes are assumed to be $A_1(0) = \sqrt{2}/\sqrt{3}$ and $A_2(0) = 1/\sqrt{3}$, which satisfy the condition $A_1(0)/A_2(0) = -V_2(\omega - \Omega_1)/[V_1(\omega - \Omega_2)]$. It can be seen that, although the probabilities $P_1(t)$, $P_2(t)$, and $P_1(t) + P_2(t)$ tend to stable periodic multioscillation as time goes on, the maximum value of $P_1(t) + P_2(t)$ in the oscillation is close to one. This shows that most of the photon is trapped near the atom. This phenomenon is more obvious in the other three figures. In contrast to the multioscillation process shown in Fig. 4(a), the oscillation in Fig. 4(b) is simple. With the given parameters in Fig. 4(b), we calculate the coefficient B_n in Eq. (31) and find that $|B_1|^2 = 0.277046$ and $|B_2|^2 = 0.722862$, which are much greater than $|B_3|^2 = 1.418 \times 10^{-6}$. So only the two bound states with energy being E_1 and E_2 play a main role in the time evolution process. It is worth noting that, when the two transition frequencies Ω_1, Ω_2 are much greater than all ω_k, most of the probabilities $P_1(t)$ and $P_2(t)$ can still remain and keep periodic oscillation with frequency being $E_1 - E_2$ even when $A_1(0)/A_2(0) \neq -V_2\Omega_1/(V_1\Omega_2)$. This is because the regime of bound-state trapping also plays an important role in this situation. From Fig. 4(b), we see that the rate of trapping can nearly become 100% under these two trapping regimes. In Fig. 4(c), we research the situation that the two transition frequencies Ω_1, Ω_2 are equal. It is found that the amplitudes $A_1(t)$ and $A_2(t)$ can always keep their initial values as long as the initial amplitudes satisfy the relation $A_1(0)/A_2(0) = -V_2/V_1$. In Fig. 4(d), we discuss the situation that ω_k are much greater than Ω_1 and Ω_2 with initial amplitudes $A_1(0)/A_2(0) = -V_2/V_1$. The evolution of populations is similar to that in Fig. 4(b). In this situation, the three coefficients are calculated as $|B_1|^2 = 3.657 \times 10^{-6}$, $|B_2|^2 = 0.808575$, and $|B_3|^2 = 0.190969$. So the two bound states with lower energy E_2, E_3 dominate the spontaneous emission process and $P_2(t)$ and $P_3(t)$ oscillate periodically with frequency being $E_2 - E_3$.

VI. EMITTED FIELD

From Eq. (31), one can see that the radiation field can be written as a sum of two parts, which come from the two terms in Eq. (31):

$$C_x(t) = \langle x, g|\Psi(t)\rangle = C_x^l(t) + C_x^p(t). \tag{39}$$

Here, $C_x^l(t)$ is associated with the discrete bound states and is expressed as

$$C_x^l(t) = \sum_n \frac{(z-\Omega_2)A_1(0) + I(z)U_1(0)}{V_1 I(z)(z-\omega)[K(z)]'} \times \frac{(z-\Omega_1)\varphi(z)}{\sqrt{1-(\frac{2J}{z-\omega})^2}} e^{-izt} e^{-|x|/l_n}\Big|_{z=E_n}, \tag{40}$$

where $\varphi(z) = (-)^{|x|\theta(z-\omega)}$ and $\theta(x)$ is the step function, which is 1 when $x > 0$ and is zero when $x < 0$. The $\sum_n$ in the expression of $C_x^l(t)$ represents the sum of terms with different discrete eigenvalues. The frequency of each term is E_n. The amplitude of each term drops exponentially as $e^{-|x|/l_n}$ when the distance from the atom increases, but does not decay with time. The size of the localized amplitude is determined by the length $l_n = -1/\log\{(1 - \sqrt{1 - [2J/(E_n - \omega)]^2})$ $|E_n - \omega|/2J\}$. When the relative energy $|E_n - \omega|$ decreases, the localized length l_n increases and the amplitude becomes more nonlocalized. As the value of $|E_n - \omega|$ decreases to $2J$, the localized length tends to infinity. In this case, the amplitude is no longer localized. As mentioned above, the population in the atom's lower level can jump to the upper levels by absorbing the localized photon. The existence of the localized field leads to the trapping of fractional populations in the upper levels.

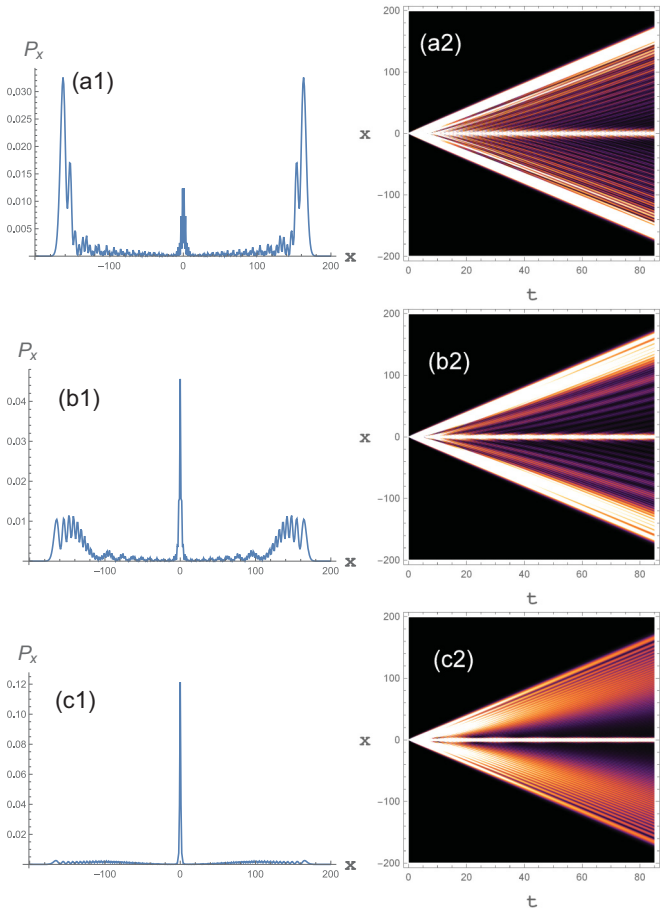

FIG. 5. Left panels are the radiation field distribution function $P_x(t)$ along the coupled-resonator waveguide at the large time $t = 85(1/J)$. The right panels are the space-time diagram of the radiation field distribution function $P_x(t)$. For (a1) and (a2), $\Omega_1/J = 0.4$, $\Omega_2/J = 0.7$; for (b1) and (b2), $\Omega_1/J = 1$, $\Omega_2/J = 1.3$; for (c1) and (c2), $\Omega_1/J = 2$, $\Omega_2/J = 3$. The other parameters are $V_1/J = 0.8$, $V_2/J = 0.2$, $\omega/J = 0$.

Now we discuss the radiation field $C_x^p(t)$, which is derived as

$$C_x^p(t) = \sum_k \frac{u_{ke_1}A_1(0) + u_{ke_2}A_2(0)}{NF_k^*} \times [e^{ikx} + r_k e^{i|kx|}]e^{-i\omega_k t}. \tag{41}$$

Obviously, $C_x^p(t)$ represents a propagating field. This propagating field travels away from the atom in the form of traveling pulses.

In Fig. 5, we plot the photon probability distribution $P_x = |C_x(t)|^2$ as a function of position and the space-time diagram

of the radiation field with different transition frequency in Figs. 5(a), 5(b) and 5(c). As time goes on, the radiation field spread from the atom to the two sides with opposite group velocities. After long enough time, part of the radiation field is trapped near around the atom. Comparing Figs. 5(a), 5(b) and 5(c). one can see that, as the frequencies Ω_1 and Ω_2 increase away from the center of the scattering energy band, the trapping of the radiation field is enhanced, which is consistent with the enhancement of the trapping of populations in the upper levels.

VII. DISCUSSION AND CONCLUSION

In this paper, we have studied the energy structure of a one-dimensional waveguide with model dispersion which is locally coupled by a three-level atom and the excitation transport dynamics in the spontaneous-emission process in this system. The system's discrete eigenvalues are given by the poles of the Green's function as shown in Eq. (30). Here, we point out that the eigenvalue equation can also be obtained by solving the time-independent Schrödinger equation $H|\Psi_n\rangle = E_n|\Psi_n\rangle$, which gives the same result as the poles of the Green's function. By numerical calculation, it is found that the number of bound states in this system is not fixed and depends on the coupling strengths and the relative position of the atom's transition frequencies from the band. The sudden change of the system's energy-level structure in the critical point reveals that there is a quantum phase transition [37–39]. The time evolution of the population in the atom's excited states and the photon probability distribution function across the waveguide are studied by expanding the system's wave function with the bound and scattering states. If one of the atom's transition frequencies and its corresponding coupling strength are taken to be the limit $\Omega_i/J, V_i/J \to 0$ ($i = 1$ or 2), the result that comes from the waveguide coupled by a two-level system will be recovered. It is worth emphasizing that the time evolution expression as shown in Eq. (31) can also be acquired by solving the time-dependent Schrödinger equation $i\hbar d|\Psi(t)\rangle/dt = H|\Psi(t)\rangle$. A detailed calculation through this method will be presented elsewhere.

By investigating the system's time evolution, we find that the radiation field can be characterized by two components: one is localized near around the atom and the other travels away from the atom. The localized field is emitted and absorbed and reemitted by the atom similar to that in vacuum Rabi oscillations; the difference is that not all population in the atom's excited take part in this oscillation. How the quantum interference between the atom's two transitions affects the radiation field is investigated, and we found that by controlling the initial amplitudes in the atom's upper levels, the determined k mode can be excluded in the emitted field. Besides, when the scattering band's width is narrow so that the scattering energy can be approximately considered to be equal to the center energy of the band or that the atom's transition frequencies are much greater than the scattering energy or the scattering energy are much greater than the atom's transition frequencies or the atom's transition frequencies are equal to each other, the population in the excited states are greatly trapped by controlling the initial amplitudes in this system.

ACKNOWLEDGMENTS

This work is supported by the National Basic Research Program of China (Grants No. 2016YFA0301201 and No. 2014CB921403), the NSFC (Grant No. 11534002), and the NSAF (Grants No. U1730449 and No. U1530401).

[1] J. T. Shen and S. Fan, Phys. Rev. Lett. **95**, 213001 (2005).
[2] L. Zhou, Z. R. Gong, Y. X. Liu, C. P. Sun, and F. Nori, Phys. Rev. Lett. **101**, 100501 (2008).
[3] H. Zheng and H. U. Baranger, Phys. Rev. Lett. **110**, 113601 (2013).
[4] H. J. Kimble, Nature (London) **453**, 1023 (2008).
[5] B. Dayan, A. S. Parkins, T. Aoki, E. P. Ostby, K. J. Vahala, and H. J. Kimble, Science **319**, 1062 (2008).
[6] L. Qiao, Phys. Rev. A **96**, 013860 (2017).
[7] D. Roy, C. M. Wilson, and O. Firstenberg, Rev. Mod. Phys. **89**, 021001 (2017).
[8] P. Facchi, S. Pascazio, F. V. Pepe, and K. Yuasa, J. Phys. Commun. **2**, 035006 (2018).
[9] D. E. Chang, A. S. Sorensen, E. A. Demler, and M. D. Lukin, Nat. Phys. **3**, 807 (2007).
[10] O. Astafiev, A. M. Zagoskin, A. A. Abdumalikov, Jr., Y. A. Pashkin, T. Yamamoto, K. Inomata, Y. Nakamura, and J. S. Tsai, Science **327**, 840 (2010).
[11] J. Claudon, J. Bleuse, N. S. Malik, M. Bazin, P. Jaffrennou, N. Gregersen, C. Sauvan, P. Lalanne, and J.-M. Gerard, Nat. Photon. **4**, 174 (2010).
[12] A. Wallraff, D. I. Schuster, A. Blais, L. Frunzio, R. S. Huang, J. Majer, S. Kumar, S. M. Girvin, and R. J. Schoelkopf, Nature (London) **431**, 162 (2004).
[13] M. J. Hartmann, F. G. S. L. Brandao, and M. B. Plenio, Nat. Phys. **2**, 849 (2006).
[14] M. Notomi, E. Kuramochi, and T. Tanabe, Nat. Photon. **2**, 741 (2008).
[15] A. A. Abdumalikov, Jr., O. Astafiev, A. M. Zagoskin, Y. A. Pashkin, Y. Nakamura, and J. S. Tsai, Phys. Rev. Lett. **104**, 193601 (2010).
[16] S. Felicetti, G. Romero, D. Rossini, R. Fazio, and E. Solano, Phys. Rev. A **89**, 013853 (2014).
[17] J. Q. Liao, Z. R. Gong, L. Zhou, Y. X. Liu, C. P. Sun, and F. Nori, Phys. Rev. A **81**, 042304 (2010).
[18] Z. H. Wang, Y. Li, D. L. Zhou, C. P. Sun, and P. Zhang, Phys. Rev. A **86**, 023824 (2012).
[19] L. Zhou, Y. Chang, H. Dong, L. M. Kuang, and C. P. Sun, Phys. Rev. A **85**, 013806 (2012).
[20] M. T. Cheng, X. S. Ma, M. T. Ding, Y. Q. Luo, and G. X. Zhao, Phys. Rev. A **85**, 053840 (2012).
[21] L. Zhou, L. P. Yang, Y. Li, and C. P. Sun, Phys. Rev. Lett. **111**, 103604 (2013).

[22] J. Lu, L. Zhou, L. M. Kuang, and F. Nori, Phys. Rev. A **89**, 013805 (2014).
[23] Z. R. Gong, H. Ian, L. Zhou, and C. P. Sun, Phys. Rev. A **78**, 053806 (2008).
[24] Z. H. Wang, L. Zhou, Y. Li, and C. P. Sun, Phys. Rev. A **89**, 053813 (2014).
[25] T. Shi and C. P. Sun, Phys. Rev. B **79**, 205111 (2009).
[26] G. Calajó, F. Ciccarello, D. Chang, and P. Rabl, Phys. Rev. A **93**, 033833 (2016).
[27] S. John and T. Quang, Phys. Rev. A **50**, 1764 (1994).
[28] P. Longo, P. Schmitteckert, and K. Busch, Phys. Rev. Lett. **104**, 023602 (2010); Phys. Rev. A **83**, 063828 (2011).
[29] S. E. Kocabas, Phys. Rev. A **93**, 033829 (2016).
[30] J. Lu, L. Zhou, H. C. Fu, and L.-M. Kuang, Phys. Rev. A **81**, 062111 (2010).
[31] M. Biondi, S. Schmidt, G. Blatter, and H. E. Türeci, Phys. Rev. A **89**, 025801 (2014).
[32] F. Lombardo, F. Ciccarello, and G. M. Palma, Phys. Rev. A **89**, 053826 (2014).
[33] E. Sánchez-Burillo, D. Zueco, L. Martín-Moreno, and J. J. García-Ripoll, Phys. Rev. A **96**, 023831 (2017).
[34] C. Cohen-Tannoudji, J. Dupont-Roc, and G. Grynberg, *Atom-Photon Interactions: Basic Processes and Applications* (Wiley, New York, 1992).
[35] E. N. Economou, *Green Functions in Quantum Physics* (Springer-Verlag, Berlin, 1979).
[36] J. R. Taylor, *Scattering Theory: The Quantum Theory of Nonrelativistic Collisions* (Dover, New York, 2006).
[37] S. Sachdev, *Quantum Phase Transitions* (Cambridge University Press, Cambridge, England, 1999).
[38] Q. J. Tong, J. H. An, H. G. Luo, and C. H. Oh, Phys. Rev. B **84**, 174301 (2011).
[39] H. Z. Shen, X. Q. Shao, G. C. Wang, X. L. Zhao, and X. X. Yi, Phys. Rev. E **93**, 012107 (2016).